On the Outage Capacity of Opportunistic Beamforming With Random User Locations

Tharaka Samarasinghe, *Member, IEEE*, Hazer Inaltekin, *Member, IEEE*, and Jamie S. Evans, *Member, IEEE*

Abstract—This paper studies the outage capacity of a network consisting of a multitude of heterogeneous mobile users and operating according to the classical opportunistic beamforming framework. The base station is located at the center of the cell, which is modeled as a disk of finite radius. The random user locations are modeled using a homogeneous spatial Poisson point process. The received signals are impaired by both fading and location dependent path loss. For this system, we first derive an expression for the beam outage probability. This expression holds for all path loss models that satisfy some mild conditions. Then, we focus on two specific path loss models (*i.e.*, an unbounded model and a more realistic bounded one) to illustrate the applications of our results. In the large system limit, where the cell radius tends to infinity, the beam outage capacity and its scaling behavior are derived for the selected specific path loss models. This paper also studies opportunistic schemes that achieve fairness among the heterogeneous users. Numerical evaluations are performed to give further insights and to illustrate the applicability of the outage capacity results even to a cell having a small finite radius.

Index Terms—Opportunistic beamforming, outage capacity, Poisson point process, random user locations, fairness.

I. INTRODUCTION

A. Background and Motivation

SINCE its inception in [1], opportunistic beamforming (OBF) has sparked a great deal of interest in the wireless communications research community as an important adaptive signaling technique that utilizes multiuser diversity and varying channel conditions to extract the full multiplexing gain available in vector broadcast channels [2]–[18]. The main advantages of OBF are threefold. It attains the sum-rate capacity with full channel state information (CSI) to a first order for large numbers of mobile users (MUs) in the network [2]. Secondly, its operation only requires partial CSI in the form of signal-

to-interference-plus-noise ratios (SINR) leading to a significant reduction in the feedback load and the latency of feedback acquisition compared to capacity achieving dirty paper precoding [19]. Finally, OBF is easy to implement, which makes it a practical communication scheme. It has been also shown that OBF is an asymptotically feedback optimal transmission strategy [6]. In this paper, we consider the classical opportunistic communication along multiple orthonormal beams in a network consisting of a multitude of heterogeneous MUs, and study the outage capacity of the resulting communication system.

In most of the existing work on OBF, the MUs are assumed to be homogeneous and equidistant from the base station (BS) [2]–[8]. Recently, works such as [9] and [10] have focussed on heterogeneous networks, which are better representations of practical communication systems where the MUs experience location dependent path loss. In [9], heterogeneous MUs are grouped into a finite number of MU classes, and the asymptotic throughput scaling of the resulting system is analyzed. In [10], each MU has its own deterministic path loss coefficient, and the authors focus on the sum rate and the individual throughput scaling while simultaneously maintaining fairness among the MUs.

Similar to [9] and [10], the signal received by a MU in this paper is impaired by both fading and the location dependent path loss. However, the path loss coefficients in this paper are random, and governed by a general path loss model $G(d)$, where d represents the distance from the BS. In this setting, the ergodic capacity achieving transmission strategy involves averaging over all channel variations. The requirement to average over location dependent and usually slowly varying path loss values questions the suitability of ergodic capacity as a performance measure for this setup [20]. Thus, we focus on the beam outage capacities as a performance metric in this paper, and obtain downlink outage performance of OBF.

B. Contributions and the Organization of the Paper

Our contributions and the paper organization are as follows. In Section II, we introduce the system model and formally define the performance measures of interest. The cell is modeled as a disk of radius D with the BS located at the center of the disk. The random MU locations are modeled using a homogeneous spatial Poisson point process (PPP) of intensity λ, and the network operates according to the classical OBF framework [2]. The received signal at a MU is impaired by both fading and path loss. We say an outage event occurs on a beam when the instantaneous rate achieved on it is less than a target rate value, and the beam outage capacity is the maximum

communication rate that can be achieved on a beam without violating a preset constraint on the outage probability.

We start our analysis by obtaining an expression for the beam outage probability for the system in consideration, which holds for all path loss models that satisfy some mild conditions. Then, we use this result to derive beam outage probabilities for specific path loss models, and obtain further insights into the downlink outage performance of OBF. In particular, we focus on two well known path loss models. Firstly, we study the unbounded power-law path loss model, which is the most common path loss model in the literature [21]–[23]. In this model, the path loss can take any value between zero and infinity. Secondly, we study a more realistic bounded path loss model, where the path loss is always less than one.

In Section IV, we consider the large system limit as D tends to infinity. Using beam outage probability expressions obtained in Section III, we study the outage capacity and its scaling behavior for each of the path loss models. To this end, we obtain expressions that can be easily used to calculate the beam outage capacity of the system of interest. We also show that for the unbounded path loss model, the beam outage capacity behaves according to $O\left(\log(\lambda)\right)$ as λ grows large. On the other hand, for the bounded path loss model, the beam outage capacity behaves according to $O\left(\log\log(\lambda)\right)$ as λ grows large, revealing a different outage capacity scaling behavior. We justify why this difference occurs: It is in fact due to the singularity at the origin in the unbounded path loss model, which makes the SINR values unbounded. As λ grows large, we are almost guaranteed to have at least one MU in the small vicinity around the BS such that its inter-beam interference is practically nulled out. For such a MU, there is only power gain coming from the fading process in the bounded case. On the other hand, in the unbounded path loss model, there is also an extra power gain coming due to the singularity at the origin, which results in different scaling behaviors.

In Section V, we consider an alternative outage measure that differs from our original outage measure depending on the time scales of the channel gain vectors and the path loss values between the BS and the MUs. For the original measure, we have considered that the channel gains and the path loss values change slowly with respect to the time scale of data transmission that takes place between the BS and MUs. This is in fact a very common assumption in the literature that uses stochastic geometric based methods to model MU/BS locations [23]–[26]. However, in a practical setting, the channel gains change much faster compared to the path loss values, which can allow us to average out the effect of fading process over the time scales of data communication. This phenomenon is captured in the new outage measure. In Section V, we extend our analysis to this alternative outage measure. We show that although closely resembling more practical communication scenarios, the new outage measure is less tractable analytically, but can be computed numerically.

A main drawback of using an opportunistic scheduling policy in its plain implementation in a heterogeneous environment is its inability to provide fairness among different MUs. If the MUs were homogeneous as in [2]–[8], fairness would be achieved as an automatic byproduct of the homogeneity

assumption. For the sake of completeness, we also focus on the outage capacity of this simpler homogeneous system model that ignores the path loss between the MU and the BS. In this context, the MUs are equidistant from the BS, and the cell radius becomes irrelevant as the effect of distance is nullified by ignoring path loss. Also, the number of MUs in the cell is now a deterministic value N. For this setting, we obtain analytical expressions for the beam outage capacity. To this end, we also show that the beam outage capacity scales according to $O\left(\log\log(N)\right)$, which is the same scaling behavior of the ergodic downlink sum-rate [2], as the number of MUs grows large. On the other hand, in the system model considered in this paper, MUs having a high path loss value, *i.e.*, cell edge MUs, will starve for data, which eliminates fairness in the system. In Section VI, we analyze the beam outage capacity of a system adhering to a CDF based scheduling technique to achieve time-wise fairness among MUs [10], [27]. In such a system, the MU having the best SINR relative to its own statistics is scheduled for data communication. This means the system will ignore the path loss values when making the scheduling decision, which gives every MU an equal opportunity of being scheduled.

In Section VII, we present numerical evaluations to provide more insights into our results. To this end, we show that the large system limit obtained by sending D to infinity closely approximates the beam outage capacity even for cells having a finite radius. Moreover, the rate of convergence of these results increases with the MU intensity and the path loss exponent. In addition, we compare the two outage measures in Section VII. We show that for a given outage probability constraint ϵ, the outage capacity will be higher if the modified outage measure in Section V is considered. This observation is however different for high ϵ values due to distinct dynamic ranges of beam SINR values obtained for different outage measures. We also focus on numerically obtaining the optimum cell radius when CDF based scheduling is used to preserve fairness in the system. Section VIII concludes the paper.

II. SYSTEM MODEL AND PROBLEM SETUP

We consider a multi-antenna single-cell vector broadcast channel. The BS is equipped with M transmitter antennas, and each MU is equipped with a single receive antenna. The cell is modeled as a disk of radius D with the BS located at the center of the disk. MUs are distributed over the plane according to a PPP Φ of intensity λ. For a particular realization of MU locations, Fig. 1 gives a graphical illustration of the part of the plane that includes the cell.

The study is based on the assumptions of Rayleigh fading and unit power noise. To this end, the random channel gains between the receive antenna of the ith MU and the transmit antennas of the BS are given by $\boldsymbol{h}_i = (h_{1,i}, \ldots, h_{M,i})^\top$, where $h_{k,i}$ is the channel gain between the kth transmit antenna at the BS and the receive antenna at the ith MU. We assume that the channel gains are independent and identically distributed (i.i.d.) random variables, each of which is drawn from a zero mean and unit variance *circularly-symmetric complex Gaussian* distribution $\mathcal{CN}(0, 1)$. The path loss values of all MUs are governed by a path loss model $G(d)$, where d is the distance from
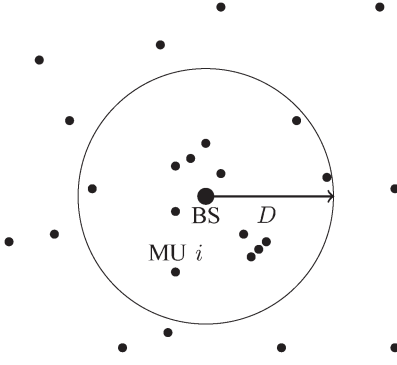
Fig. 1.   The network model for a particular realization of MU locations.

the BS. Therefore, the random path loss values are also i.i.d. among the MUs, where the randomness stems from the fact that MU locations are random. The path loss model is general in the sense that G can be any function that is continuous, positive, non-increasing, and $G(d) = O(d^{-\alpha})$ as d grows large for some $\alpha > 2$.[1] In addition, we assume a quasi-static block fading model over time. For the sake of notational simplicity, we drop the time index here in the channel model, and also later in the representation of transmitted and received signals.

The network operates according to the classical OBF framework [2]. The BS transmits M different data streams intended for M different MUs. The symbols of the kth stream are represented by s_k. They are chosen from the capacity achieving unit power (complex) Gaussian codebooks, and are sent along the directions of M orthonormal beamforming vectors $\{\boldsymbol{b}_k = (b_{1,k}, \ldots, b_{M,k})^\top\}_{k=1}^M$. The overall transmitted signal from the BS is given by

$$s = \sqrt{\rho} \sum_{k=1}^M \boldsymbol{b}_k s_k, \tag{1}$$

where ρ is the transmit power per beam. The signal received by the ith MU is given by

$$Y_i = \sqrt{g_i} \boldsymbol{h}_i^\top \boldsymbol{s} + Z_i, \tag{2}$$

where g_i is the path loss coefficient between the ith MU and BS, Z_i is the $\mathcal{CN}(0,1)$ additive background noise.

Let $\text{SINR}_{m,i}$ be the SINR value corresponding to the mth beam at the ith MU. Then, it is given by

$$\text{SINR}_{m,i} = \frac{\left| \boldsymbol{h}_i^\top \boldsymbol{b}_m \right|^2}{(\rho g_i)^{-1} + \sum_{k=1, k \neq m}^M \left| \boldsymbol{h}_i^\top \boldsymbol{b}_k \right|^2}. \tag{3}$$

Unlike [2], for given MU locations, the beam SINR values are no longer identically distributed among the MUs, due to the location dependent path loss. Let $F_i(x)$ represent the cumulative distribution function (CDF) of the beam SINR at MU i. Using techniques similar to those used in [2], it is not

hard to show that $F_i(x)$, for a given path loss value $g_i = g$, is written as

$$F_i(x|g_i = g) = 1 - \frac{e^{-\frac{x}{g\rho}}}{(x+1)^{M-1}} \tag{4}$$

for all i (*i.e.*, replace ρ in (15) of [2] with ρg). The probability distribution function (PDF) for a given path loss value $g_i = g$ is written as,

$$f_i(x|g_i = g) = \frac{e^{-\frac{x}{g\rho}}}{(x+1)^M} \left[\frac{1}{g\rho}(x+1) + M - 1 \right]. \tag{5}$$

Since the MU locations are modeled using a PPP, and since G is non-increasing, the CDF of the path loss of a MU can be written as

$$\mathcal{G}(g) = 1 - \left[\frac{G^{-1}(g)}{D} \right]^2. \tag{6}$$

Here, we define $G^{-1}(g)$ as $G^{-1}(g) = \inf\{d : G(d) \leq g\}$. We note that this definition allows jump discontinuities in $\mathcal{G}(g)$. An example of such a path loss model is given in Section VII.

Each MU feeds back its SINR information to the BS along an error free feedback link, and the BS selects the MU with the highest SINR on each beam to maximize the communication rate. Let N be the random number of MUs in the cell. The instantaneous rate on beam m (measured in terms of nats/s/Hz) can be written as

$$r_m = \log \left(1 + \max_{1 \leq i \leq N} \text{SINR}_{m,i} \right), \tag{7}$$

and $r_m = 0$ when the maximization is over the null set, *i.e.*, when $N = 0$. When characterizing the instantaneous rate, the channel gain vectors, the path loss values and the number of MUs are considered to be random quantities. Then, by using fundamental concepts of outage [20], we formally define our first outage measure, which we call *type*-1 outage,[2] as follows.

Definition 1: A *type*-1 outage event occurs on beam m when the instantaneous rate achieved on the beam r_m is less than a target rate value x, *i.e.*, when $r_m \leq x$.

Directly following from this definition, we have the beam outage probability, or the CDF of the rate on a beam

$$\Omega_1(x) = \Pr\{r_m \leq x\} = F^\star(e^x - 1), \tag{8}$$

where $F^\star$ is the CDF of the maximum SINR on a beam. This expression will be instrumental in obtaining expressions for the beam outage capacities of the system of interest, which we formally define as follows.

Definition 2: The beam outage capacity for *type*-1 outage $C_1(\epsilon)$ is defined as the supremum of communication rates on a beam that results in an outage probability of less than ϵ for that particular beam, *i.e.*,

$$C_1(\epsilon) = \sup \{x : \Omega_1(x) \leq \epsilon\}, \tag{9}$$

for $\epsilon \in (0, 1)$.

---

[1]The variable d in $G(d)$ is actually normalized by a reference distance D_{ref}. Typical distances for D_{ref} are on the order of a kilometer for macrocells, of hundred meters for pico/microcells and of several meters for femtocells [28]. d takes the same units as D_{ref}. In the current paper, and in most related other works in the literature, it is assumed that $D_{\text{ref}} = 1$ unit distance. Therefore, both λ and D can be considered normalized unitless quantities in this paper.

[2]We also define a slightly different outage measure in Section V, which we call *type*-2 outage.

In the remaining parts of the paper, we will focus on obtaining expressions for Ω_1, which will be used to analyze beam outage capacities of the system model of interest.

III. BEAM OUTAGE PROBABILITIES

In this section, we will obtain expressions for beam outage probabilities for the system of interest. We will first obtain expressions considering the general path loss model that was introduced in Section II, and then apply the results to specific path loss models to obtain further insights.

A. Beam Outage Probabilities for General Path Loss Models

In our setup, the number of MUs in the cell N is a Poisson distributed random variable with mean $\lambda \pi D^2$. Hence, in order to derive beam outage probabilities, we will first condition on N and path loss values, and then we will remove conditioning by averaging over the location process. These ideas are formally presented in the following theorem.

Theorem 1: For a given communication rate x, the beam outage probability $\Omega_1(x)$ is equal to $F^\star(e^x - 1)$, where $F^\star(x)$ is given by

$$F^\star(x) = \exp\left(\frac{-\lambda\pi}{(x+1)^{M-1}} \int_0^{D^2} \exp\left(\frac{-x}{G(\sqrt{t})\rho} \right) dt \right). \quad (10)$$

Proof: Conditioning on N and $\boldsymbol{g} = (g_1, \ldots, g_N)^\top$, we have $F^\star(x|N, \boldsymbol{g}) = \prod_{i=1}^N F_i(x|g_i)$, where $\boldsymbol{g}$ is the vector containing the path loss values of all the MUs in the cell. Averaging over the i.i.d. path loss values gives us $F^\star(x|N) = \left(\int_{G(D)}^{G(0)} F(x|v) d\mathcal{G}(v) \right)^N$. Similarly, by observing that $\Pr\{N = n\} = (e^{-\lambda\pi D^2}(\lambda\pi D^2)^n/n!)$, we can uncondition on the number of MUs, and obtain

$$F^\star(x) = \sum_{n=0}^{\infty} \frac{e^{-\lambda\pi D^2}(\lambda\pi D^2)^n}{n!} \left(\int_{G(D)}^{G(0)} F(x|v) d\mathcal{G}(v) \right)^n.$$

Now, by using (4), we have

$$F^\star(x) = \sum_{n=0}^{\infty} \frac{e^{-\lambda\pi D^2}(\lambda\pi D^2)^n}{n!}$$
$$\times \left(\int_{G(D)}^{G(0)} d\mathcal{G}(v) - \int_{G(D)}^{G(0)} \frac{e^{\frac{-x}{v\rho}}}{(x+1)^{M-1}} d\mathcal{G}(v) \right)^n.$$

Since $\int_{G(D)}^{G(0)} d\mathcal{G}(v) = 1$, we get

$$F^\star(x) = \exp\left(-\lambda\pi D^2 \int_{G(D)}^{G(0)} \frac{e^{\frac{-x}{v\rho}}}{(x+1)^{M-1}} d\mathcal{G}(v) \right)$$

by writing the infinite summation using the exponential function. Substituting for $\mathcal{G}(v)$ from (6) and making a variable change $(G^{-1}(v))^2 = t$ completes the proof. ∎

For a given communication rate x, the beam outage probability can be obtained numerically by means of (10). However, further analytical characterization of the outage capacity shedding light on the system performance using this expression is not straightforward due to the integral that depends on the path loss model. Therefore, in the next subsection, we apply this result to derive beam outage probabilities for specific path loss models.

B. Beam Outage Probabilities for Specific Path Loss Models

First, we focus on the classical unbounded path loss model, which is $G(d) = d^{-\alpha}$, where $\alpha > 2$, *e.g.*, see [21]–[23]. The following lemma gives us the beam outage probability expression for this case.

Lemma 1: Let $G(d) = d^{-\alpha}$, where $\alpha > 2$. For a given communication rate x, the beam outage probability $\Omega_{1,\text{ub}}(x)$ is equal to $F_{\text{ub}}^\star(e^x - 1)$, where $F_{\text{ub}}^\star(x)$ is given by

$$F_{\text{ub}}^\star(x) = \exp\left(\frac{-2\lambda\pi}{\alpha(x+1)^{M-1}} \left(\frac{\rho}{x} \right)^{\frac{2}{\alpha}} \gamma\left(\frac{2}{\alpha}, \frac{xD^\alpha}{\rho} \right) \right), \quad (11)$$

and $\gamma(\cdot)$ is the lower incomplete gamma function.

Proof: From Theorem 1, we have

$$F_{\text{ub}}^\star(x) = \exp\left(\frac{-\lambda\pi}{(x+1)^{M-1}} \int_0^{D^2} \exp\left(\frac{-xt^{\frac{\alpha}{2}}}{\rho} \right) dt \right),$$

and evaluating the integral completes the proof [29]. ∎

The above path loss model has been extensively used in the literature due to its mathematical tractability. However, this model has an unrealistic singularity at the origin, which might lead to flawed conclusions [26], [30]. Therefore, we also obtain the beam outage probability for a more realistic bounded gain path loss model. To this end, we choose $G(d)$ as $G(d) = (1 + d^\alpha)^{-1}$, where $\alpha > 2$, *e.g.*, see [26], [30], [31].

Lemma 2: Let $G(d) = (1 + d^\alpha)^{-1}$, where $\alpha > 2$. For a given communication rate x, the beam outage probability $\Omega_{1,\text{b}}(x)$ is equal to $F_{\text{b}}^\star(e^x - 1)$, where $F_{\text{b}}^\star(x)$ is given by

$$F_{\text{b}}^\star(x) = \exp\left(\frac{-2\lambda\pi e^{\frac{-x}{\rho}}}{\alpha(x+1)^{M-1}} \left(\frac{\rho}{x} \right)^{\frac{2}{\alpha}} \gamma\left(\frac{2}{\alpha}, \frac{xD^\alpha}{\rho} \right) \right), \quad (12)$$

and $\gamma(\cdot)$ is the lower incomplete gamma function.

Since the proof follows from the same lines of the proof of Lemma 1, we skip it to avoid repetitions. It can be seen that (12) differs from (11) due to an extra $e^{-x/\rho}$ term in (12). It is this extra term that changes the behavior of the outage capacity fundamentally in the bounded path loss case, and leads to an interesting result on the scaling behavior of the beam outage capacity, which will be studied in detail in the next section.

IV. BEAM OUTAGE CAPACITY AND ITS SCALING BEHAVIOR

For the analysis in this section, we will focus on the large system limit as D tends to infinity. When $D \to \infty$,

$\gamma((2/\alpha), (xD^\alpha/\rho))$ converges to $\Gamma(2/\alpha)$. Therefore, for the large system limit, (11) and (12) can be written as

$$\bar{F}^\star_{\mathrm{ub}}(x) = \exp\left(\frac{-2\lambda\pi}{\alpha(x+1)^{M-1}}\left(\frac{\rho}{x}\right)^{\frac{2}{\alpha}}\Gamma\left(\frac{2}{\alpha}\right)\right) \quad (13)$$

$$\bar{F}^\star_{\mathrm{b}}(x) = \exp\left(\frac{-2\lambda\pi e^{\frac{-x}{\rho}}}{\alpha(x+1)^{M-1}}\left(\frac{\rho}{x}\right)^{\frac{2}{\alpha}}\Gamma\left(\frac{2}{\alpha}\right)\right), \quad (14)$$

respectively. By using Definition 2, and the monotonicity of $F^\star$, for *type*-1 outage, the beam outage capacity can be written as

$$C_1(\epsilon) = \log\left(F^{\star^{-1}}(\epsilon) + 1\right), \quad (15)$$

where $F^{\star^{-1}}(\epsilon) = \inf\{x : F^\star(x) \geq \epsilon\}$. We will first obtain beam outage capacity and its scaling behavior for the unbounded path loss model through the following theorem.

Theorem 2: Let $y^\star$ be the solution of

$$y^{a+1} - y^a - \left(\frac{-b}{\log\epsilon}\right)^{\frac{\alpha}{2}} = 0, \quad (16)$$

where $a = (\alpha/2)(M-1)$, $b = (2\lambda\pi/\alpha)\Gamma(2/\alpha)\rho^{2/\alpha}$ and $y \in (1, \infty)$. Then, for $G(d) = d^{-\alpha}$, $\alpha > 2$, the beam outage capacity $C_{1,\mathrm{ub}}(\epsilon)$ in the large system limit is equal to $\log(y^\star)$. Moreover, $C_{1,\mathrm{ub}}(\epsilon)$ scales according to $O(\log(\lambda))$ as the MU intensity λ grows large.

Proof: See Appendix A. ∎

According to Theorem 2, we can obtain the beam outage capacity by using a root finding algorithm to find the unique $y^\star$ solving (16) for any value of M. Further, when $M = 1$, we can get a closed form expression for the beam outage capacity as

$$C_{1,\mathrm{ub}}(\epsilon) = \log\left(1 + \rho\left(\frac{-2\lambda\pi\Gamma\left(\frac{2}{\alpha}\right)}{\alpha\log\epsilon}\right)^{\frac{\alpha}{2}}\right).$$

The beam outage capacity expression above for $M = 1$ clearly indicates the logarithmic outage capacity scaling with λ.

Next, we will obtain similar results for the bounded gain path loss model.

Theorem 3: Let $y^\star$ be the solution of

$$\log\left(y^a(y-1)\right) + \frac{\alpha}{2\rho}(y-1) - \frac{\alpha}{2}\log\left(\frac{-b}{\log\epsilon}\right) = 0, \quad (17)$$

where $a = (\alpha/2)(M-1)$, $b = (2\lambda\pi/\alpha)\Gamma(2/\alpha)\rho^{2/\alpha}$ and $y \in (1, \infty)$. Then, for $G(d) = (1 + d^\alpha)^{-1}$, $\alpha > 2$, the beam outage capacity $C_{1,\mathrm{b}}(\epsilon)$ in the large system limit is equal to $\log(y^\star)$. Moreover, $C_{1,\mathrm{b}}(\epsilon)$ scales according to $O(\log\log(\lambda))$ as the MU intensity λ grows large.

Proof: See Appendix A. ∎

Similar to the unbounded case, we can use a common root finding algorithm on (17) to find the beam outage capacity when $G(d) = (1 + d^\alpha)^{-1}$. More interestingly, Theorem 3 reveals a different outage capacity scaling behavior than that of Theorem 2. This difference in scaling is in fact caused by the singularity at the origin in the unbounded path loss model. When $M = 1$, it is easy to see that the SNR values become unbounded in the unbounded path loss model, which in turn

leads to different scaling behaviors. For $M > 1$, we are almost guaranteed to have at least one MU in the small vicinity δ of the BS such that its inter-beam interference is practically nulled out, for large values of λ as a function of δ (*i.e.*, opportunistic nulling). For such a MU, there is only power gain coming from the fading process in the bounded case. On the other hand, in the unbounded path loss model, there is also an extra power gain coming due to the singularity at the origin, which results in different scaling behaviors. These issues are investigated more rigorously in Appendix A.

V. OUTAGE CAPACITY FOR MULTI-TIME SCALE FADING

In this section, we consider an alternative outage measure that differs from our original outage measure given in Definition 1 depending on the time scales of the channel gain vectors and the path loss values between the BS and the MUs. For *type*-1 outage, we have considered the communication scenario in which both $\boldsymbol{h}_i$ and g_i change slowly with respect to the time scale of data transmission that takes place between the BS and MU i, for all $i \in \{1, \dots, N\}$. This is in fact a very common assumption in the literature that uses stochastic geometric based methods to model MU/BS locations [23]–[26]. However, in a practical setting, the channel gain vector $\boldsymbol{h}_i$ can change rapidly over time scales smaller than the time scale of communication, which can allow us to obtain ergodic data rates averaged over $\boldsymbol{h}_i$. Considering this phenomenon, we introduce another outage measure, which we call *type*-2 outage, and define it formally as follows.

Definition 3: A *type*-2 outage event occurs on beam m when the average rate achieved on the beam for a given set of MU locations is less than a target rate value x, *i.e.*, when $\mathsf{E}[r_m|N, \boldsymbol{g}] \leq x$, where $\boldsymbol{g} = (g_1, \dots, g_N)^\top$ and r_m is given in (7).

We recall that r_m is a function of the channel gain vectors, the path loss values of the MUs, and the number of MUs. For *type*-1 outage, we use r_m directly to characterize the outage probability, but for *type*-2 outage, we first average r_m over the channel gain vectors, and use the resulting ergodic rate to characterize the outage probability. Thus, there is a subtle difference in obtaining the CDF of the rate on a beam for each type of outage. To this end, for *type*-1 outage, we calculate $\Pr\{r_m \leq x\} = \mathsf{E}[\Pr\{r_m \leq x|N, \boldsymbol{g}\}]$. On the other hand, for *type*-2 outage we calculate $\Pr\{\mathsf{E}[r_m|N, \boldsymbol{g}] \leq x\}$.

Along these ideas, we have the beam outage probability, or the CDF of the rate on a beam

$$\Omega_2(x) = \Pr\left\{\mathsf{E}[r_m|N, \boldsymbol{g}] \leq x\right\}$$

$$= \mathsf{E}\left[\Pr\left\{\int_0^\infty \log(1+t)dF^\star(t|N, \boldsymbol{g}) \leq x \,\middle|\, N\right\}\right].$$

Also, we have $F^\star(t|N, \boldsymbol{g}) = \prod_{i=1}^N F_i(t|g_i)$. Therefore,

$$\Omega_2(x) = \Pr\left\{\sum_{i=1}^N \int_0^\infty \log(1+t)f_i(t|g_i)\prod_{k=1, k\neq i}^N F_k(t|g_k)dt \leq x\right\}. \quad (18)$$

Using Definition 2, we can write the beam outage capacity as

$$C_2(\epsilon) = \sup\{x : \Omega_2(x) \leq \epsilon\}, \quad (19)$$

for $\epsilon \in (0,1)$. Due to the complex form of $\Omega_2(x)$ appearing in (19), it is not possible to write down a simplified expressions for C_2 as we have done for C_1. Numerical evaluation is tractable, but not straightforward as in the *type*-1 outage case as well (more details will be provided in Section VII). Therefore, although being more closer to the practical scenario, the new outage measure is less tractable analytically, which is in fact the reason behind the aforementioned common assumption regarding the time scales of fading and path loss processes with respect to that of data transmission. We note that since the number of MUs in the cell is Poisson distributed, $\Omega_2(x)$ can also be written as,

$$\Omega_2(x) = \sum_{n=0}^{\infty} \frac{e^{-\lambda\pi D^2}(\lambda\pi D^2)^n}{n!}$$

$$\times \Pr\left\{\sum_{i=1}^{n}\int_0^{\infty} \log(1+t)f_i(t|g_i)\prod_{k=1,k\neq i}^{n} F_k(t|g_k)dt \leq x\right\}. \quad (20)$$

However, due to the infinite summation in (20), (18) turns out to be more useful when evaluating C_2 numerically. Next, we will analyze a pressing concern for a system consisting of heterogeneous MUs, which is achieving fairness.

VI. TIME-WISE FAIR SCHEDULING OF MOBILE USERS

A main drawback of using an opportunistic scheduling policy in its plain implementation in a heterogeneous environment is its inability to provide fairness among different MUs. If the MUs were homogeneous (equidistant from the BS), which is the most common system model for OBF in the literature [1]–[3], [5], [9], fairness would be achieved as an automatic byproduct of the homogeneity assumption. For the sake of completeness, we will provide an outage capacity analysis for this simpler model in Appendix C. On the other hand, in a heterogeneous setup, MUs having a high path loss value, *i.e.*, cell edge MUs, will starve for data, which eliminates fairness in the system.

The fairness among MUs can be defined by using two different view points. The first one is providing the same rate for all the MUs, which we call rate-wise fairness. The second one is providing all the MUs with an equal share of the channel in time, which we call time-wise fairness. In this paper, we will only focus on time-wise fairness. There are three main methods of achieving time-wise fairness for a set of heterogeneous MUs in the OBF literature. The first one is to use the proportionally fair algorithm when scheduling the MUs [1]. As a second option, the system can use selective feedback techniques to achieve fairness in the network [5], [9]. Finally, the time-wise fairness can also be achieved by using CDF based scheduling techniques [10], [27].

In this section, we will analyze the beam outage capacity of a system adhering to a CDF based scheduling technique to achieve fairness among MUs. In such a system, the scheduler knows the SINR distributions of all the MUs, *i.e.*, $F_i(x|g_i)$ for all $i \in \{1,\ldots,N\}$ for any given N. For a particular beam m, the scheduler calculates the probabilities $p_{m,i} = F_i(\text{SINR}_{m,i}|g_i)$ for all i. We note that these probabilities are i.i.d. random variables, uniformly distributed between zero and one. Then, it schedules transmission to the MU $i_m^\star$ having the highest probability value, *i.e.*, $i_m^\star = \arg\max_{1\leq i\leq N} p_{m,i}$. This means that the system will communicate with the MU having the best SINR relative to its own statistics, or the system will ignore the path loss values for the scheduling decision and will schedule the MU doing the best in terms of fading. Since the system takes the path loss values into consideration when calculating the probabilities, all the MUs have an equal chance of being scheduled. The instantaneous rate on a beam (measured in terms of nats/s/Hz) can be written as

$$r_{m,\text{fair}} = \log(1 + \text{SINR}_{m,i_m^\star}). \quad (21)$$

We will first obtain an expression for the CDF of the SINR on a beam of the scheduled MU through the following lemma.

Lemma 3: Consider an OBF system adhering to a CDF based scheduling scheme. Then, if the number of MUs in the cell N and the path loss vector containing path loss values of all MUs $\boldsymbol{g}$ are given, the CDF of the SINR on any beam is given by

$$F_{\text{fair}}(x|N,\boldsymbol{g}) = \frac{1}{N}\sum_{i=1}^{N}[F_i(x|g_i)]^N. \quad (22)$$

Proof: See Appendix B. ∎

A. Fairness Considering Type-1 Outage

We will first focus on *Type*-1 outage and we will use the result in Lemma 3 to study the outage capacity of the system of interest. To this end, the CDF of the rate on a beam can be written as

$$\Omega_{1,\text{fair}}(x) = F_{\text{fair}}(e^x - 1). \quad (23)$$

Similar to the analysis in Section III, in order to derive beam outage probabilities, we will remove conditioning of $F_{\text{fair}}(x|N,\boldsymbol{g})$ given in Lemma 3 by averaging over the location process. These ideas are formally presented in the following theorem.

Theorem 4: For a given communication rate x, the beam outage probability $\Omega_{1,\text{fair}}(x)$ of a system operating based on CDF based scheduling is equal to $F_{\text{fair}}(e^x - 1)$, where $F_{\text{fair}}(x)$ is given by

$$F_{\text{fair}}(x) = \frac{1}{D^2}\int_0^{D^2} \exp\left(\frac{-\lambda\pi D^2}{(x+1)^{M-1}}e^{\frac{-x}{G(\sqrt{t})\rho}}\right)dt. \quad (24)$$

Proof: See Appendix B. ∎

Unlike the results obtained in Theorem 1 for the greedy scheduling policy, the application of the results in Theorem 4 for specific path loss models does not result in further simplification of the expression. However, the resulting expressions can

be easily evaluated numerically. Next we will focus on *Type*-2 outage.

B. Fairness Considering Type-2 Outage

For *type*-2 outage, the CDF of the rate on a beam is given by

$$\Omega_{2,\text{fair}}(x) = \Pr\left\{\int_0^\infty \log(1+t)dF_{\text{fair}}(t|N,\boldsymbol{g}) \le x\right\}.$$

By using Lemma 3,

$$\Omega_{2,\text{fair}}(x) = \Pr\left\{\frac{1}{N}\sum_{i=0}^N \int_0^\infty \log(1+t)d\left[F_i(t|g_i)\right]^N \le x\right\}.$$

For *type*-2 outage, similar to the greedy scheduling policy considered in Section V, it is hard to further simplify the expression obtained for $\Omega_{2,\text{fair}}(x)$ to a form that facilitates analysis.

It is important to note that for both outage measures, the SINR value of a MU will decrease as it moves away from the BS due to path loss. Therefore, when making D large, the SINR values of the cell edge MUs go to zero, resulting in zero rate for the cell edge MUs. Since all MUs are considered equally for scheduling to preserve fairness, the rate achieved goes to zero as $D \to \infty$. In fact, for *type*-1 outage, this can be seen through direct inspection of (24), where D being finite is a necessity for the derived CDF expression to have meaningful values. In the next section, we will provide some further insights into the results obtained in this paper through numerical evaluations.

VII. NUMERICAL EVALUATIONS

We will start by giving a graphical illustration of beam outage probabilities as a function of target communication rates x for each of the path loss models in Fig. 2. We can see that the unbounded model achieves a better beam outage probability with a larger dynamic range because the path loss gain in this case can take any value between zero and infinity. Also, the beam outage probability curves shift right with increasing values of λ, illustrating the multiuser diversity gains analyzed in Theorems 2 and 3. When comparing *type*-1 outage with *type*-2 outage, we can see that *type*-1 outage has a larger dynamic range. This is because, according to Definition 3, the randomness of the fading process is averaged out when obtaining Ω_2. Due to this averaging, we can also see that beam outage probabilities are better for *type*-2 outage compared to its counterpart. This means, for a given ϵ, the outage capacity will be higher if *type*-2 outage is considered. This observation is however different for high target communication rates, as shown in the figure, due to the lower dynamic range of Ω_2. Having compared the beam outage probabilities and the beam outage capacities for the above two different definitions of outage, we will only focus on *type*-1 outage, which is the main focus of this paper, in the remaining part of this section to avoid repetitions. Similar conclusions continue to hold qualitatively for the type-2 outage measure as well.

In Section IV, we have focused on the large system limit as D tends to infinity. Therefore, the beam outage capacity results
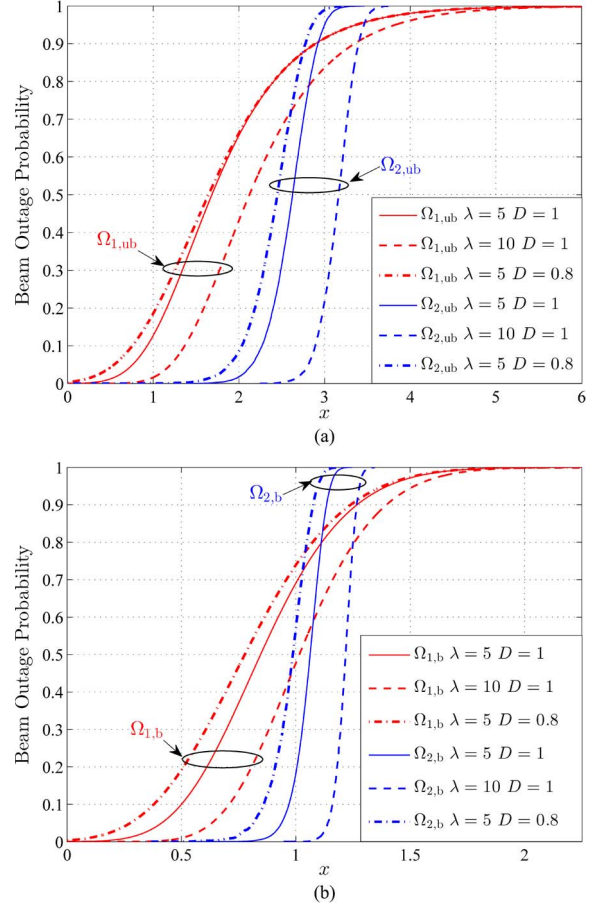

Fig. 2. Graphical illustration of beam outage probabilities for different values of λ and D, where $\rho = 1$, $M = 2$, and $\alpha = 4$. (a) Unbounded path loss model. (b) Bounded path loss model.

in Theorems 2 and 3 are true for a cell of infinite radius. By using the results in Lemmas 1 and 2, we can also numerically evaluate the beam outage capacity for a cell of finite radius. The probability of a MU at the cell edge having the maximum SINR on any beam decreases with the cell radius, due to the path loss. Therefore, intuitively, the beam outage capacity results in the large system limit should closely approximate the finite case after some value of D. To this end, Fig. 3(a) illustrates the behavior of the beam outage capacity as a function of the cell radius. In this figure, $C_{1,\text{ub}}(\epsilon, D)$ and $C_{1,\text{b}}(\epsilon, D)$ represent the beam outage capacities of the unbounded (*i.e.*, $G(d) = d^{-\alpha}$) and bounded (*i.e.*, $G(d) = (1 + d^{-\alpha})^{-1}$) path loss models for finite D, respectively. It is shown in the figure that the beam outage capacity in the large system limit closely approximates the beam outage capacities even for small finite values of D. D does not need to be very large for the results to match, and the large system beam outage capacities are very close to those achieved in cells having a radius of more than one.

Furthermore, we can observe that the convergence is faster for the unbounded path loss model in Fig. 3(a). In both models, there is a high probability of a MU staying close to the BS being scheduled for communication. However, this probability is comparatively higher in the unbounded model due to the unbounded gain. Therefore, its dependence on the cell radius is less prominent compared to the bounded one, leading to the
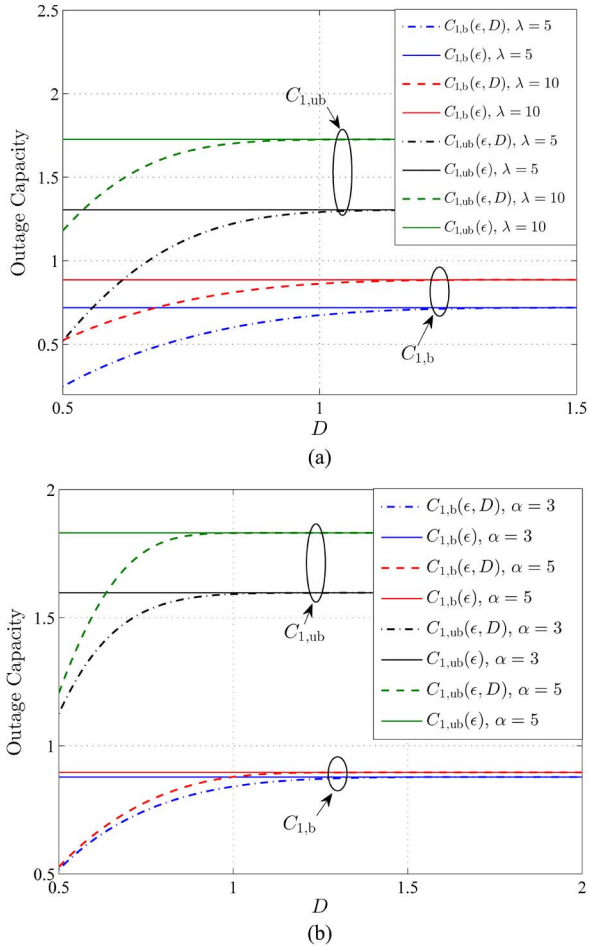
(a)

(b)

Fig. 3. The behavior of the beam outage capacity with the cell radius for *type*-1 outage, where $\rho = 1$, $\epsilon = 0.1$, and $M = 2$. (a) For different values of λ, $\alpha = 4$. (b) For different values of α, $\lambda = 10$.

faster convergence behavior. Secondly, a faster convergence can be observed with increasing values of λ as well. Increasing λ increases the number of MUs per unit area, which includes the number of MUs staying close to the BS. This again makes the cell edge MUs less prominent, causing faster convergence. By observing (11) and (12), we can expect the rate of convergence to increase with α as well. This is illustrated in Fig. 3(b). This result is also expected intuitively because increasing α increases the path loss at cell edge MUs, making them less prominent.

Next, we focus on the scaling behavior of the beam outage capacity, which is illustrated in Fig. 4. We can clearly observe the difference in scaling behaviors, *i.e.*, $O\left(\log(\lambda)\right)$ for the unbounded model, and $O\left(\log\log(\lambda)\right)$ for the bounded model, which are in line with the results in Theorems 2 and 3. It is interesting to note that when λ is relatively small, the beam outage capacity first decreases with α, and then increases with α when λ is large. The decrease with α is rather intuitive because increasing α increases the path loss, which decreases the SINR and the rate. However, note that when $d < 1$, $G(d)$ increases with α. As mentioned earlier, when we increase λ, more prominence is given to the MUs staying close to the BS, *i.e.*, to the MUs having distance less than one. Therefore, at high values of λ, the beam outage capacity increases with α.
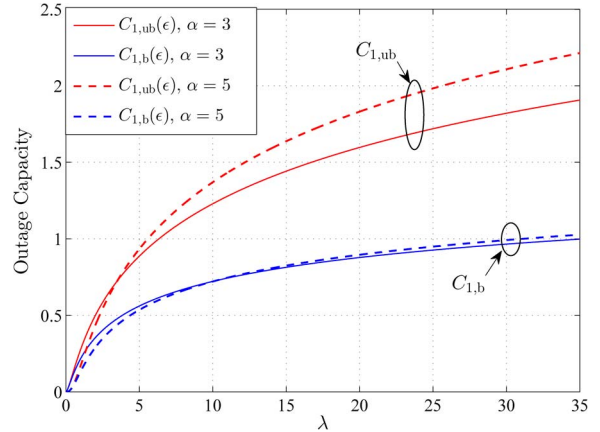

Fig. 4. The behavior of the beam outage capacity with the MU intensity, where $\rho = 1$, $\epsilon = 0.01$, and $M = 2$.

This somewhat counter intuitive behavior is especially more pronounced for the unbounded path loss model. To overcome it in the bounded case, one can use a path loss model taking the form of $G(d) = \max(d_0, d)^{-\alpha}$, where d_0 is a constant that accounts for a guard zone around the BS up to a certain distance. $G(d) = (1 + d)^{-\alpha}$ is another option. Due to the generality of the path loss model definition in Section II, and the result obtained in Theorem 1, our analysis can be easily extended to both of these path loss models.

Now, we will focus on achieving fairness in the network through CDF based scheduling. Obviously providing fairness will necessitate a sacrifice in terms of rate. This difference in rates will depend on the radius of the cell. Selecting the optimum cell radius for the fair scheduling scheme is another interesting research problem, whose solution will lead to an important design parameter for wireless operators. To this end, our numerical results are presented in Fig. 5. The system will gain through multiuser diversity when λ, D or both are increased. Therefore, the outage capacity first increases with D for fixed λ. However, the outage capacity starts to decrease after a certain threshold value $D^\star$, which is the optimum cell radius. The SINR values of cell edge MUs decrease with the cell radius due to path loss. Since all the MUs are considered equally for scheduling to preserve fairness, the rate reduction caused by the reduction of the SINR values of cell edge MUs outperforms the multiuser diversity gain for $D > D^\star$. $D^\star$ decreases with λ as increasing λ allows the BS to achieve the same multiuser diversity gain with a cell having a smaller radius. $D^\star$ decreases with α as well since increasing α decreases the SINR at cell edge MUs. Also, $D^\star$ achieved for the unbounded path loss model is less than the $D^\star$ achieved for the bounded path loss model since the unbounded model gives more prominence to the MUs located close to BS.

The CDF of the SINR on a beam in a multi-cell environment is readily available in the literature [13], [15], [32] and similar techniques used in this paper can be utilized to study the outage capacity in a multi-cell environment. However, the expression obtained for the aforementioned CDF is more complex compared to the single cell scenario, which makes the analysis much less tractable mathematically. Some insights on these related multi-cell extensions can be found in [32].
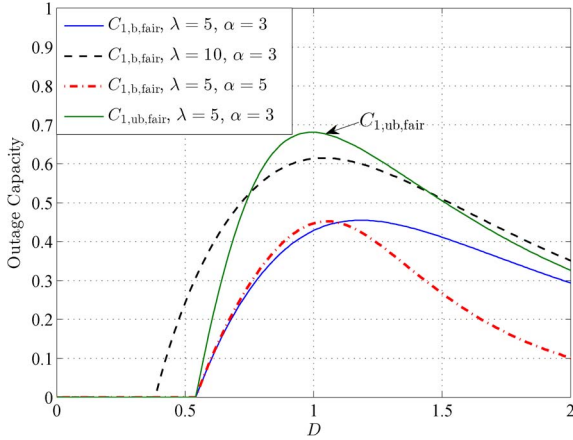
Fig. 5. The change of the beam outage capacity with the cell radius for the CDF based scheduling scheme, where $\rho = 1$, $\epsilon = 0.01$, and $M = 2$.

VIII. CONCLUSION

In this paper, we have studied the outage capacity of a network consisting of a multitude of mobile users whose random locations are modeled using a homogeneous spatial Poisson point process, and operating according to the classical opportunistic beamforming framework. Considering a cell modeled as a disk of radius D, we have first obtained an expression for the beam outage probability. This expression holds for all path loss models that satisfy some mild conditions. Then, we have applied this result to two well known path loss models. Firstly, we have considered the classical unbounded path loss model, which is $G(d) = d^{-\alpha}$, where $\alpha > 2$ and d represents the distance from the base station. Secondly, we have considered a more realistic bounded gain path loss model $G(d) = (1 + d^\alpha)^{-1}$, where $\alpha > 2$. Then, in a large system setting where D tends to infinity, we have obtained results for the beam outage capacity and its scaling behavior, for each of these path loss models. To this end, we have obtained expressions that can be easily used to calculate the beam outage capacity of the system of interest. We have shown that the beam outage capacity behaves according to $O\left(\log(\lambda)\right)$ for the unbounded model, and according to $O\left(\log\log(\lambda)\right)$ for the bounded model, as the user intensity λ grows large. The difference is due to the unrealistic singularity in the unbounded model at $d = 0$.

We have also analyzed the beam outage capacity of a system adhering to a CDF based scheduling technique to achieve timewise fairness among the heterogeneous users. An alternative outage measure that differs from our original outage measure depending on the time scales of the channel gain vectors and the path loss values between the BS and the users has been also considered in the analysis. We have also provided extensive numerical evaluations to give further insights into our analytical results. To this end, we have shown that the large system limit closely approximates the beam outage capacity even for cells having a finite radius. We have illustrated numerically how to obtain the optimum cell radius when the CDF based scheduling scheme is used to preserve fairness in the system. This result is of practical importance for wireless operators to determine optimum cell sizes for opportunistic wireless communication.

APPENDIX A
BEAM OUTAGE CAPACITY

A. Proof of Theorem 2

We will only focus on the $M > 1$ case. $M = 1$ case follows from the same lines. From (8), (15), and (13), the beam outage capacity $C_{1,\mathrm{ub}}(\epsilon)$ should satisfy

$$\left(\frac{-b}{\log \epsilon}\right)^{\frac{\alpha}{2}} = e^{aC_{1,\mathrm{ub}}(\epsilon)}\left(e^{C_{1,\mathrm{ub}}(\epsilon)} - 1\right)$$

as $D \to \infty$. Setting $e^{C_{1,\mathrm{ub}}}(\epsilon) = y$ gives us (16). It is not hard to show that $y^{a+1} - y^a - (-b/\log\epsilon)^{\alpha/2}$ is a strictly increasing function of y that tends to infinity as y grows large, and is negative as y approaches to one. Therefore, $y^\star$ is unique, and its logarithm gives the beam outage capacity of the system without any ambiguity.

Also, from (16),

$$\log\left([y^\star]^a[y^\star - 1]\right) = \log\left(\left[\frac{-b}{\log \epsilon}\right]^{\frac{\alpha}{2}}\right)$$

$$\Rightarrow \log y^\star = \frac{\alpha}{2a}\log\lambda - \frac{1}{a}\log(y^\star - 1) + O(1)$$

$$= \frac{\alpha}{2a}\log\lambda - \frac{1}{a}\left[\log y^\star + \log\left(1 - \frac{1}{y^\star}\right)\right] + O(1)$$

$$= \frac{\alpha}{2(a+1)}\log\lambda + O(1).$$

This final equation indicates that $\log y^\star$ scales according to $O(\log(\lambda))$, which further implies $C_{1,\mathrm{ub}}(\epsilon)$ scales according to $O(\log(\lambda))$ as λ grows large.

B. Proof of Theorem 3

From (8), (15), and (14), the beam outage capacity $C_{1,\mathrm{b}}(\epsilon)$ should satisfy

$$\left(\frac{-b}{\log \epsilon}\right)^{\frac{\alpha}{2}} = e^{aC_{1,\mathrm{b}}(\epsilon) + \frac{\alpha}{2\rho}\left(e^{C_{1,\mathrm{b}}(\epsilon)} - 1\right)}\left(e^{C_{1,\mathrm{b}}(\epsilon)} - 1\right)$$

as $D \to \infty$. Taking logarithm of both sides and setting $e^{C_{1,\mathrm{b}}}(\epsilon) = y$ give us (17). It is not hard to show that this is a strictly increasing function of y that tends to infinity as y grows large, and is negative as y approaches to one. Therefore, $y^\star$ is unique, and its logarithm gives the beam outage capacity of the system without any ambiguity.

Also, from (17), similar to the proof of Theorem 2,

$$y^\star = \rho\log\lambda - \frac{2\rho a}{\alpha}\log y^\star - \frac{2\rho}{\alpha}\log(y^\star - 1) + O(1)$$

$$= \rho\log\lambda - \frac{2\rho(a+1)}{\alpha}\log y^\star - \frac{2\rho}{\alpha}\log\left(1 - \frac{1}{y^\star}\right) + O(1)$$

$$= \rho\log\lambda - \frac{2\rho(a+1)}{\alpha}\log\log\lambda + O(1).$$

Therefore, $y^\star$ scales according to $O\left(\log(\lambda)\right)$, which implies that $C_{1,\mathrm{b}}(\epsilon)$ scales according to $O\left(\log\log(\lambda)\right)$ as λ grows large.

C. Difference in Scaling Behavior

Let $B(\delta)$ be the disk with radius δ around the BS. The SINR value corresponding to beam m at MU i given in (3) can be alternatively written as

$$\text{SINR}_{m,i} = \frac{X_{m,i}}{(\rho g_i)^{-1} + \sum_{j=1, j\neq m}^{M} X_{j,i}},$$

where $X_{j,i}$, $j \neq m$, represents inter-beam interference from beam j at MU i. In our set-up, $X_{j,i}$'s are exponentially distributed with unit mean.

Define the event $A(\delta)$ as

$$A(\delta) = \left\{ \exists i \in \Phi \bigcap B(\delta) \ \& \ \sum_{j=1, j\neq m}^{M} X_{j,i} \leq \delta^{\alpha} \ \& \ X_{m,i} \geq 1 \right\}.$$

Let $\text{SINR}_m^{\star} = \max_{i \in \Phi} \text{SINR}_{m,i}$ denote the maximum SINR on beam m. On event $A(\delta)$, we have $\text{SINR}_m^{\star} \geq (1/\delta^{\alpha}(\rho^{-1} + 1))$, which implies $r_m \geq -\alpha \log(\delta) - \log(1 + \rho^{-1})$ on $A(\delta)$.

We will now show that $\Pr(A(\delta))$ can be made arbitrarily close to 1 by choosing λ large enough. To this end, let $\Pr\{\sum_{j=1, j\neq m}^{M} X_{j,i} \leq \delta^{\alpha}\} = p_1$ and $\Pr\{X_{m,i} \geq 1\} = p_2$. The first term represents the *opportunistic nulling* of interference, and the second term controls the direct channel gain of the ith MU. Then,

$$\Pr(A(\delta)) = \sum_{n=0}^{\infty} \frac{e^{-\lambda\pi\delta^2}(\lambda\pi\delta^2)^n}{n!} \left(1 - (1 - p_1 p_2)^n\right)$$

$$= 1 - e^{-\lambda\pi\delta^2 p_1 p_2}.$$

We can lower bound p_1 as

$$p_1 \geq \Pr\left\{X_{j,i} \leq \frac{\delta^{\alpha}}{M-1}\right\}^{M-1} = \left(1 - e^{-\frac{\delta^{\alpha}}{M-1}}\right)^{M-1}$$

$$= O(\delta^{\alpha}) \text{ as } \delta \to 0.$$

p_2 is equal to $p_2 = e^{-1}$. Hence, by choosing λ such that $\lambda\pi\delta^2 = \delta^{-\alpha-\epsilon}$, for some small $\epsilon > 0$, we have $\Pr(A(\delta)) \geq 1 - e^{-O(\delta^{-\epsilon})} \to 1$ as $\delta \to 0$. Therefore, we have $r_m \geq (\alpha/(\alpha + 2 + \epsilon)) \log(\lambda) + O(1)$ with high probability as λ tends to infinity. This implies beam outage capacity scales according to $\log(\lambda)$.

The conclusion is that as λ tends to infinity, we can, with *high* probability, find a MU in a small disk of radius $(\pi\lambda)^{(-1/(\alpha+2+\epsilon))}$ around the BS such that interference at this MU is opportunistically nulled out (*i.e.*, smaller than $(\pi\lambda)^{(-\alpha/(\alpha+2+\epsilon))}$), and therefore we observe a path loss gain of $\lambda^{(\alpha/(\alpha+2+\epsilon))}$ effectively.

APPENDIX B
BEAM OUTAGE PROBABILITIES FOR TIME-WISE FAIR SYSTEMS

A. Proof of Lemma 3

Since beams are symmetric, it is enough to focus only on beam m. Recall that $p_{m,i}$ represent the level of $\text{SINR}_{m,i}$ relative

to its own statistics. Since $p_{m,i} = F_i(\text{SINR}_{m,i}|g_i)$, we have

$$F_{\text{fair}}(x|N, \boldsymbol{g}) = \Pr\{\text{SINR}_{m,i_m^{\star}} \leq x|N, \boldsymbol{g}\}$$

$$= \sum_{i=1}^{N} \Pr\{\text{SINR}_{m,i} \leq x, i_m^{\star} = i|N, \boldsymbol{g}\}$$

$$= \sum_{i=1}^{N} \Pr\{p_{m,i} \leq F_i(x|g_i), p_{m,j} \leq p_{m,i}, \forall j|N, \boldsymbol{g}\},$$

$$F_{\text{fair}}(x|N, \boldsymbol{g}) = \sum_{i=1}^{N} \int_{0}^{F_i(x|g_i)} \Pr\{p_{m,i} = t|N, \boldsymbol{g}\}$$

$$\Pr\{p_{m,j} \leq t, \forall j \neq i|N, \boldsymbol{g}, p_{m,i} = t\} dt.$$

Since $p_{m,i}$'s are independent and uniformly distributed over [0, 1], $\Pr\{p_{m,i} = t|N, \boldsymbol{g}\} = 1$, and

$$\Pr\{p_{m,j} \leq t, \forall j \neq i|N, \boldsymbol{g}, p_{m,i} = t\} = \prod_{j \neq i} \Pr\{p_{m,j} \leq t|N, \boldsymbol{g}\}$$

$$= t^{N-1}.$$

Thus,

$$F_{\text{fair}}(x|N, \boldsymbol{g}) = \sum_{i=1}^{N} \int_{0}^{F_i(x|g_i)} t^{N-1} dt = \frac{1}{N} \sum_{i=1}^{N} [F_i(x|g_i)]^N.$$

which completes the proof.

B. Proof of Theorem 4

Averaging $F_{\text{fair}}(x|N, \boldsymbol{g})$ given in Lemma 3 over the i.i.d. path loss values gives us

$$F_{\text{fair}}(x|N) = \frac{1}{N} \int_{G(D)}^{G(0)} \sum_{i=1}^{N} [F_i(x|v)]^N \, d\mathcal{G}(v)$$

$$= \int_{G(D)}^{G(0)} [F(x|v)]^N \, d\mathcal{G}(v).$$

Similarly, by observing that $\Pr\{N=n\} = (e^{-\lambda\pi D^2}(\lambda\pi D^2)^n/n!)$, we can uncondition on the number of MUs, and obtain

$$F_{\text{fair}}(x) = \sum_{n=0}^{\infty} \frac{e^{-\lambda\pi D^2}(\lambda\pi D^2)^n}{n!} \left(\int_{G(D)}^{G(0)} [F(x|v)]^n \, d\mathcal{G}(v)\right)$$

$$= e^{-\lambda\pi D^2} \left(\int_{G(D)}^{G(0)} \sum_{n=0}^{\infty} \frac{(\lambda\pi D^2 F(x|v))^n}{n!} d\mathcal{G}(v)\right).$$

Now, by writing the infinite summation using the exponential function, and by using (4), we have

$$F_{\text{fair}}(x) = \int_{G(D)}^{G(0)} \exp\left(\frac{-\lambda\pi D^2}{(x+1)^{M-1}} e^{\frac{-x}{v\rho}}\right) d\mathcal{G}(v).$$

Using the expression given for $\mathcal{G}(v)$ in (6) and making a variable change $(G^{-1}(v))^2 = t$ completes the proof.

Appendix C
Outage Capacity Analysis for Equidistant Mobile Users

The model with equidistant MUs [2] ignores the path loss between the MU and the BS, or alternatively considers the path loss value between each MU and BS to be deterministic and equal to a fixed number. This implies that the received SINR values on a beam are i.i.d. among the MUs. In this context, the radius of the cell becomes irrelevant since the effect of distance is nullified by setting fixed path loss values. In this simpler model, it is also considered that the number of MUs N is a fixed integer. Our earlier analysis can be extended readily to provide outage capacities for this case as well, which is illustrated below.

If the path loss value between each MU and the BS is fixed at $\bar{g}$, we have,

$$F^\star(x) = [F(x)]^N = \left[1 - \frac{e^{-\frac{x}{\bar{g}\rho}}}{(x+1)^{M-1}} \right]^N. \quad (25)$$

By using (25) and (15), we can obtain analytical expressions for the outage capacity of a system consisting a multitude of equidistant MUs. These expressions can also be used to derive results for the scaling behavior of the outage capacity as the number of MUs grows large. The results are formally stated in the following theorem.

Theorem 5: The beam outage capacity $C_{1,\mathrm{ed}}(\epsilon)$ for N equidistant MUs is equal to

$$C_{1,\mathrm{ed}}(\epsilon) = \log \left(\bar{g}\rho(M-1)\mathrm{W} \left(\frac{e^{\frac{1}{(M-1)\bar{g}\rho}}}{(M-1)\bar{g}\rho} \left(1 - \epsilon^{\frac{1}{N}} \right)^{\frac{1}{1-M}} \right) \right)$$

if $M \geq 2$, and $C_{1,\mathrm{ed}}(\epsilon) = \log(1 - \bar{g}\rho \log(1 - \epsilon^{1/N}))$ if $M = 1$, where W is the Lambert W function given by the defining equation $\mathrm{W}(x)\exp(\mathrm{W}(x)) = x$ for $x \geq -(1/e)$. Moreover, $C_{1,\mathrm{ed}}(\epsilon)$ scales according to $O\left(\log\log(N)\right)$ as the number of MUs N grows large.

Proof: Using (25), we have $F^{\star -1}(x) = F^{-1}(x^{1/N})$. From [5],

$$F^{-1}(x) = -1 + (M-1)\rho\mathrm{W} \left(\frac{e^{\frac{1}{(M-1)\rho}}}{(M-1)\rho}(1-x)^{\frac{1}{1-M}} \right)$$

for $M \geq 2$, and $F^{-1}(x) = -\rho\log(1-x)$ for $M = 1$. Thus, we can readily obtain $F^{\star -1}(x)$ by substituting $x^{1/N}$ in these expressions given for $F^{-1}(x)$. $C_{1,\mathrm{ed}}(\epsilon)$ follows from using $F^{\star -1}(x)$ in (15).

As N grows large,

$$\log \left(1 - \epsilon^{\frac{1}{N}} \right) = \log \left(1 - e^{\frac{\log \epsilon}{N}} \right) = \log \left(\frac{\log \epsilon}{N} + O \left(\frac{1}{N^2} \right) \right)$$

$$= \log \left(\frac{\log \epsilon}{N} \right) + \log \left(1 + O \left(\frac{1}{N} \right) \right)$$

$$= -\log N + O(1).$$

Now, considering $M = 1$, as N grows large

$$C_{1,\mathrm{ed}}(\epsilon) = \log \left(\bar{g}\rho \log N + O(1) \right) = \log\log N + O(1).$$

Therefore, $C_{1,\mathrm{ed}}(\epsilon)$ scales according to $O\left(\log\log(N)\right)$ when $M = 1$.

For $M \geq 2$, as N grows large

$$C_{1,\mathrm{ed}}(\epsilon) = \log \left(\mathrm{W} \left(\frac{e^{\frac{1}{(M-1)\rho}}}{(M-1)\rho} \left(1 - \epsilon^{\frac{1}{N}} \right)^{\frac{1}{1-M}} \right) \right) + O(1).$$

By taking the logarithm on both sides in $\mathrm{W}(x)\exp(\mathrm{W}(x)) = x$, we have $\mathrm{W}(x) = \log(x) - \log(\mathrm{W}(x))$. Since $\log(1 - \epsilon^{1/N}) = -\log N + O(1)$,

$$C_{1,\mathrm{ed}}(\epsilon) = \log \left(\frac{1}{M-1}\log(N) + O\left(\log\log(N)\right) \right) + O(1).$$

Therefore, $C_{1,\mathrm{ed}}(\epsilon)$ scales according to $O\left(\log\log(N)\right)$ for $M \geq 2$, which completes the proof. ∎

The outage capacity of a system consisting of N equidistant MUs can be easily computed by using Theorem 5. According to the theorem, the outage capacity scales according to $O\left(\log\log(N)\right)$, which is the same scaling behavior of the ergodic downlink sum-rate [2], as the number of MUs grows large.

References

[1] P. Viswanath, D. Tse, and R. Laroia, "Opportunistic beamforming using dumb antennas," *IEEE Trans. Inf. Theory*, vol. 48, no. 6, pp. 1277–1294, Jun. 2002.

[2] M. Sharif and B. Hassibi, "On the capacity of MIMO broadcast channels with partial side information," *IEEE Trans. Inf. Theory*, vol. 51, no. 2, pp. 506–522, Feb. 2005.

[3] M. Pugh and B. D. Rao, "Reduced feedback schemes using random beamforming in MIMO broadcast channels," *IEEE Trans. Signal Process.*, vol. 58, no. 3, pp. 1821–1832, Mar. 2010.

[4] J. Diaz, O. Simeone, and Y. Bar-Ness, "Asymptotic analysis of reduced-feedback strategies for MIMO Gaussian broadcast channels," *IEEE Trans. Inf. Theory*, vol. 54, no. 3, pp. 1308–1316, Mar. 2008.

[5] T. Samarasinghe, H. Inaltekin, and J. S. Evans, "Optimal selective feedback policies for opportunistic beamforming," *IEEE Trans. Inf. Theory*, vol. 59, no. 5, pp. 2897–2913, May 2013.

[6] A. Bayesteh and A. Khandani, "Asymptotic analysis of the amount of CSI feedback in MIMO broadcast channels," *IEEE Trans. Inf. Theory*, vol. 58, no. 3, pp. 1612–1629, Mar. 2012.

[7] M. Kountouris, D. Gesbert, and T. Salzer, "Enhanced multiuser random beamforming: Dealing with the not so large number of users case," *IEEE J. Sel. Areas Commun.*, vol. 26, no. 8, pp. 1536–1545, Oct. 2008.

[8] R. Couillet, J. Hoydis, and M. Debbah, "Random beamforming over quasi-static and fading channels: A deterministic equivalent approach," *IEEE Trans. Inf. Theory*, vol. 58, no. 10, pp. 6392–6425, Oct. 2012.

[9] T. Samarasinghe, H. Inaltekin, and J. S. Evans, "The feedback-capacity tradeoff for opportunistic beamforming under optimal user selection," *Perform. Eval.*, vol. 70, no. 7/8, pp. 472–492, Jul. 2013.

[10] Y. Huang and B. D. Rao, "Random beamforming with heterogeneous users and selective feedback: Individual sum rate and individual scaling laws," *IEEE Trans. Wireless Commun.*, vol. 12, no. 5, pp. 2080–2090, May 2013.

[11] H. Ju and R. Zhang, "A novel mode switching scheme utilizing random beamforming for opportunistic energy harvesting," *IEEE Trans. Wireless Commun.*, vol. 13, no. 4, pp. 2150–2162, Apr. 2014.

[12] J.-H. Li and H.-J. Su, "Opportunistic feedback reduction for multiuser MIMO broadcast channel with orthogonal beamforming," *IEEE Trans. Wireless Commun.*, vol. 13, no. 3, pp. 1321–1333, Mar. 2014.

[13] H. D. Nguyen, R. Zhang, and H. T. Hui, "Multi-cell random beamforming: Achievable rate and degrees of freedom region," *IEEE Trans. Signal Process.*, vol. 61, no. 14, pp. 3532–3544, Jul. 2013.

[14] Y. Xuezhi, J. Wei, and B. Vucetic, "A random beamforming technique for omnidirectional coverage in multiple-antenna systems," *IEEE Trans. Veh. Technol.*, vol. 62, no. 3, pp. 1420–1425, Mar. 2013.

[15] Y. Huang and B. D. Rao, "Reducing feedback requirements of the multiple weight opportunistic beamforming scheme via selective multiuser diversity," in *Proc. IEEE Veh. Technol. Conf.*, Las Vegas, NV, USA, Sep. 2013, pp. 1–5.

[16] C. Kim, S. Lee, and J. Lee, "SINR and throughput analysis for random beamforming systems with adaptive modulation," *IEEE Trans. Wireless Commun.*, vol. 12, no. 4, pp. 1460–1471, Apr. 2013.

[17] J. Park, H. Lee, and S. Lee, "MIMO broadcast channels based on SINR feedback using a non-orthogonal beamforming matrix," *IEEE Trans. Commun.*, vol. 60, no. 9, pp. 2534–2545, Sep. 2012.

[18] S. A. M. Xia and Y. Wu, "Non-orthogonal opportunistic beamforming: Performance analysis and implementation," *IEEE Trans. Wireless Commun.*, vol. 11, no. 4, pp. 1424–1433, Apr. 2012.

[19] G. Caire and S. Shamai, "On the achievable throughput of a multiantenna Gaussian broadcast channel," *IEEE Trans. Inf. Theory*, vol. 49, no. 7, pp. 1691–1706, Jul. 2003.

[20] D. N. C. Tse and P. Viswanath, *Fundamentals of Wireless Communications*. Cambridge, U.K.: Cambridge Univ. Press, 2005.

[21] E. S. Sousa and J. A. Silvester, "Optimum transmission ranges in a direct sequence spread spectrum multihop packet radio network," *IEEE J. Sel. Areas Commun.*, vol. 8, no. 5, pp. 762–771, Jun. 1990.

[22] E. S. Sousa, "Performance of a spread spectrum packet radio network in a Poisson field of interferers," *IEEE Trans. Inf. Theory*, vol. 38, no. 6, pp. 1743–1754, Nov. 1992.

[23] J. G. Andrews, F. Baccelli, and R. K. Ganti, "A tractable approach to coverage and rate in cellular networks," *IEEE Trans. Commun.*, vol. 59, no. 11, pp. 3122–3134, Nov. 2011.

[24] H. S. Dhillon, R. K. Ganti, F. Baccelli, and J. G. Andrews, "Modeling and analysis of K-tier downlink heterogeneous cellular networks," *IEEE J. Sel. Areas Commun.*, vol. 30, no. 3, pp. 550–560, Apr. 2012.

[25] H. ElSawy, E. Hossain, and M. Haenggi, "Stochastic geometry for modeling, analysis, design of multi-tier and cognitive cellular wireless networks: A survey," *IEEE Commun. Surveys Tuts.*, vol. 15, no. 3, pp. 996–1019, Jul. 2013.

[26] T. Samarasinghe, H. Inaltekin, and J. S. Evans, "On optimal downlink coverage in Poisson cellular networks with power density constraints," *IEEE Trans. Commun.*, vol. 62, no. 4, pp. 1382–1392, Feb. 2014.

[27] D. Park, H. Seo, H. Kwon, and B. G. Lee, "Wireless packet scheduling based on the cumulative distribution function of user transmission rates," *IEEE Trans. Commun.*, vol. 53, no. 11, pp. 1919–1929, Nov. 2005.

[28] J. G. Andrews, H. Claussen, M. Dohler, S. Rangan, and M. C. Reed, "Femtocells: Past, present, future," *IEEE J. Sel. Areas Commun.*, vol. 30, no. 3, pp. 497–508, Apr. 2012.

[29] I. Gradshteyn and I. Ryzhik, *Table of Integrals, Series, Products*, 7th ed. New York, NY, USA: Academic, 2007.

[30] H. Inaltekin, M. Chiang, H. V. Poor, and S. B. Wicker, "On unbounded path-loss models: Effects of singularity on wireless network performance," *IEEE J. Sel. Areas Commun.*, vol. 27, no. 7, pp. 1078–1092, Sep. 2009.

[31] T. Samarasinghe, H. Inaltekin, and J. S. Evans, "Optimal SNR-based coverage in Poisson cellular networks with power density constraints," in *Proc. Australian Commun. Theory Workshop*, Adelaide, SA, Australia, Jan. 2013, pp. 105–110.

[32] M. Wang, T. Samarasinghe, and J. S. Evans, "Transmission rank selection for opportunistic beamforming with quality of service constraints," in *Proc. Int. Conf. Commun.*, Sydney, NSW, Australia, Jun. 2014, pp. 1910–1915.

Tharaka Samarasinghe (S'11–M'13) was born in Colombo, Sri Lanka, in 1984. He received the B.Sc. degree in engineering from the Department of Electronics and Telecommunication Engineering, University of Moratuwa, Moratuwa, Sri Lanka, in 2008, where he received the award for the most outstanding undergraduate upon graduation. He received the Ph.D. degree from the Department of Electrical and Electronic Engineering, University of Melbourne, Melbourne, Vic., Australia, in 2012. Since September 2012, he has been with the Department of Electrical and Computer Systems Engineering, Monash University, Australia, where he is currently a Research Fellow. His research interests are in communications theory, information theory, and wireless communications networks.

Hazer Inaltekin (S'04–M'06) received the B.S. degree (High Hons.) in electrical and electronics engineering from Bogazici University, Istanbul, Turkey, in 2001, and the M.S. and Ph.D. degrees in electrical and computer engineering from Cornell University, Ithaca, NY, USA, in 2006. He is an Associate Professor of electrical and electronics engineering with Antalya International University, Antalya, Turkey. From 2006 to 2007, he was a Postdoctoral Research Associate with Cornell University, and from 2007 to 2009, with Princeton University, Princeton, NJ, USA. In 2009, he joined the Department of Electrical and Electronic Engineering, University of Melbourne as a Research Fellow. Between January 2011 and August 2011, he was a Senior Research Fellow at the same department. Since August 2011, he has been on the Faculty at Antalya International University. His research interests include wireless communications, wireless networks, social networks, game theory, and information theory.

Jamie S. Evans (S'93–M'98) was born in Newcastle, Australia, in 1970. He received the B.S. degree in physics and the B.E. degree in computer engineering from the University of Newcastle, Callaghan, N.S.W., Australia, in 1992 and 1993, respectively, where he received the University Medal upon graduation. He received the M.S. and Ph.D. degrees in electrical engineering from the University of Melbourne, Melbourne, Vic., Australia, in 1996 and 1998, respectively, and was awarded the Chancellor's Prize for excellence for his Ph.D. thesis. From March 1998 to June 1999, he was a Visiting Researcher with the Department of Electrical Engineering and Computer Science, University of California, Berkeley, CA, USA. He returned to Australia to take up a position as a Lecturer with the University of Sydney, Australia, where he stayed until July 2001. From July 2001 until March 2012, he was with the Department of Electrical and Electronic Engineering, University of Melbourne. He is currently a Professor with the Department of Electrical and Computer Systems Engineering, Monash University, Australia. His research interests are in communications theory, information theory, and statistical signal processing with a focus on wireless communications networks.